In the World of the Observer

B. F. Riley

The numerical value of any measurement outcome is mapped by any function of the observer's choosing onto integers and fractions of a denomination of the observer's choosing. Measurement outcomes that are closely related in the mind of the observer result in symmetrically related integers and fractions. From the totality of measurements, the observer apprehends a self-consistent reality ruled by theories believed by the observer.

1 Introduction

Expressed in units of the observer's choosing, measurement outcomes assume numerical values, a, equal to integer, half-integer, quarter-integer etc powers of π, π/2 and e, integer powers being favoured: $a = \pi^{n_1}$, $a = (\pi/2)^{n_2}$ and $a = e^{n_3}$ [1]. That is, the functions $f(a) = \ln(a)/\ln(\pi)$, $g(a) = \ln(a)/\ln(\pi/2)$ and $h(a) = \ln(a)$ map a onto three numbers: $n_1 = \ln(a)/\ln(\pi)$; $n_2 = \ln(a)/\ln(\pi/2)$; and $n_3 = \ln(a)$, each of which takes a value equal to an integer, half-integer, quarter-integer etc.

First, we investigate whether measurement outcomes, when expressed in units of the observer's choosing, assume numerical values equal to integer, half-integer, quarter-integer etc powers of any base of the observer's choosing. Second, we investigate whether measurement outcomes, when expressed in units of the observer's choosing, assume numerical values that map by way of any function of the observer's choosing onto integers, half-integers, quarter-integers etc. Third, we investigate whether measurement outcomes assume numerical values that map onto integers and fractions of a denomination chosen by the observer.

Two arbitrarily-chosen functions f_1 and f_2 are applied to the numerical value a of each measurement outcome to produce two numbers n_1 and n_2 ($f_1(a) = n_1$ and $f_2(a) = n_2$) which are plotted one against the other. For each set of measurements a rough idea of the maximum values of the two numbers enables the observer to choose suitable major units for the graph. The minor units are chosen before calculating the precise values of n_1 and n_2. Using two functions generates special locations on the graphs, called intersections, where n_1 and n_2 both take near-integer values.

2 Distances and lengths

For the measurements considered in this section we apply the functions $f_1(d) = \ln(d)/\ln(2.2)$ and $f_2(d) = \ln(d)/\ln(3.3)$ to the numerical value d of a distance or length measured in metres to produce the numbers $n_1 = \ln(d)/\ln(2.2)$ and $n_2 = \ln(d)/\ln(3.3)$, i.e. $d = (2.2)^{n_1}$ and $d =$

$(3.3)^{n_2}$. The bases 2.2 and 3.3 have been chosen arbitrarily. Progressively smaller distance and length scales are considered.

Values of n_1 and n_2 have first been calculated for the measured distances from Earth of the Large Magellanic Cloud (LMC: 179,000 lyr; 1.693×10^{21} m), the Small Magellanic Cloud (SMC: 210,000 lyr; 1.987×10^{21} m) and the Canis Major Dwarf Galaxy (CMD: 25,000 lyr; 2.365×10^{20} m), the latter being the nearest galaxy to the Milky Way. Distances in light years (lyr) have been taken from [2]. The numbers n_1 and n_2 calculated for the three galaxies are plotted one against the other in Figure 1. The markers lie on a straight line since n_1 and n_2 are in constant ratio. The value of n_1 for the LMC equals 62. The values of n_2 for the two Magellanic Clouds are arranged symmetrically about the number 41 at the intersection (62, 41). The value of n_1 for the CMD is equal to a half-integer (59.5).

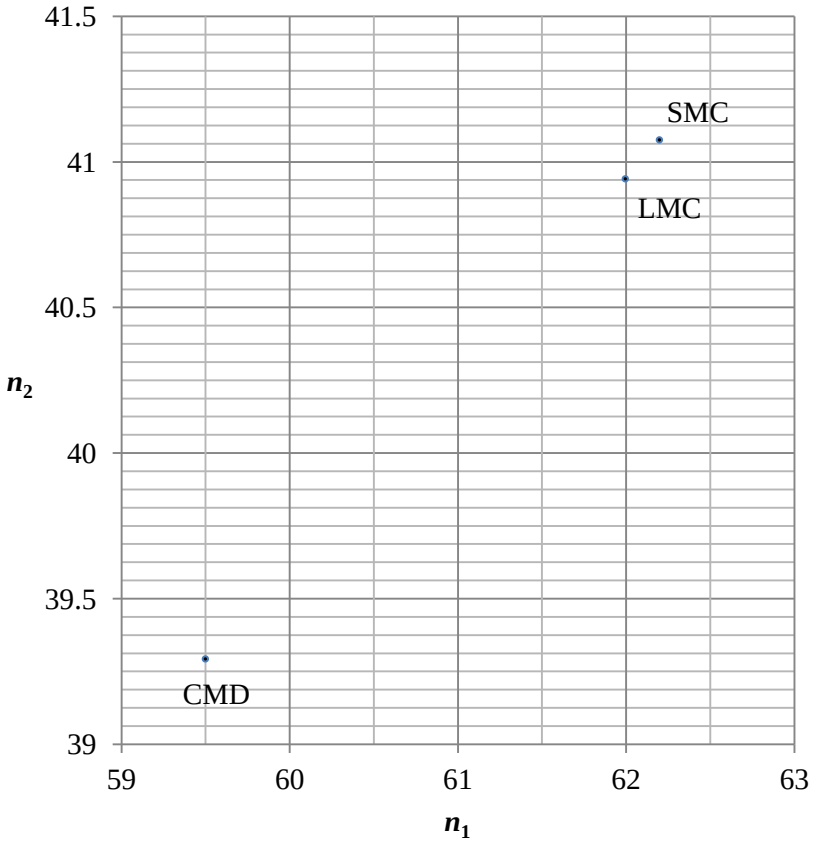

Figure 1: Values of n_1 and n_2 calculated from the distances d (in metres) from Earth of the Large Magellanic Cloud (LMC, 179,000 lyr), the Small Magellanic Cloud (SMC, 210,000 lyr) and the Canis Major Dwarf (CMD, 25,000 lyr), where $n_1 = \ln(d) / \ln(2.2)$ and $n_2 = \ln(d) / \ln(3.3)$, i,e. $d = (2.2)^{n_1}$ and $d = (3.3)^{n_2}$.

One star has been considered: Proxima Centauri, the nearest star to Earth at a distance of 4.25 lyr (4.02×10^{16} m). We see in Figure 2 that the value of n_1 is approximately equal to a half-integer (48.5), the point (n_1, n_2) being located at the intersection (48.5, 32).

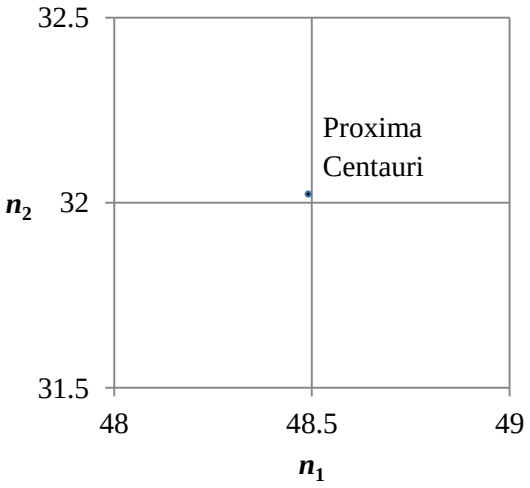

Figure 2: Values of n_1 and n_2 calculated from the distance d (in metres) from Earth of Proxima Centauri (4.25 lyr), where $n_1 = \ln(d) / \ln(2.2)$ and $n_2 = \ln(d) / \ln(3.3)$.

Values of n_1 and n_2 have been calculated for the distance by air from London (LHR) to New York (JFK, 5555 km) and then for the distance by air from LHR to San Francisco (SFO, 8638 km). The air distances have been taken from [3]. The value of n_2 for LHR - JFK equals 13, as shown in Figure 3. The point (n_1, n_2) for LHR - SFO lies on the intersection (20.25, 13.375).

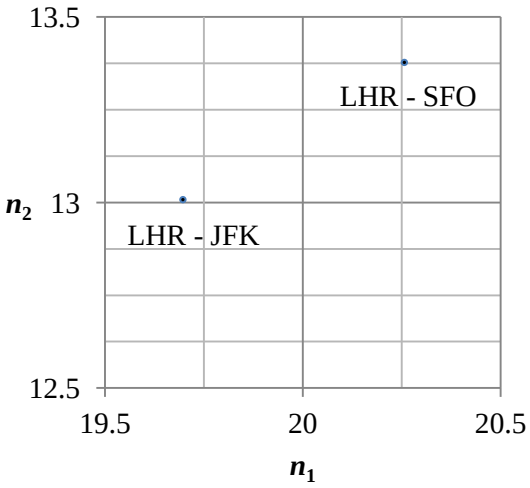

Figure 3: Values of n_1 and n_2 calculated from the distances d (in metres) by air from London (LHR) to New York (JFK, 5555 km) and from LHR to San Francisco (SFO, 8638 km), where $n_1 = \ln(d) / \ln(2.2)$ and $n_2 = \ln(d) / \ln(3.3)$.

The value of n_1 for the Marathon (42.195 km) equals a half-integer (13.5), as shown in Figure 4. The point (n_1, n_2) is located at the intersection (13.5, 9).

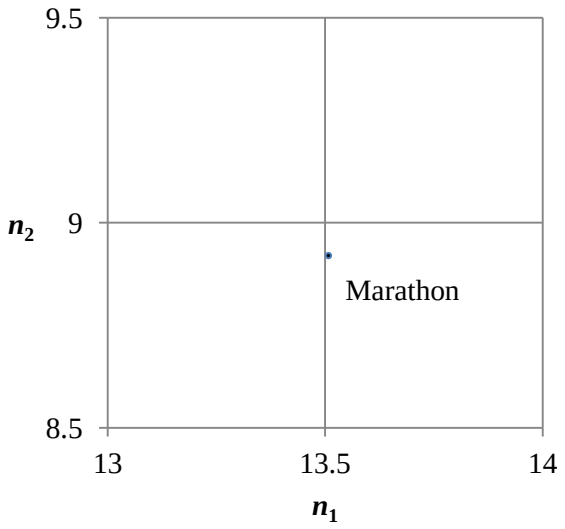

Figure 4: Values of n_1 and n_2 calculated from the length l (in metres) of the Marathon (42.195 km), where $n_1 = \ln(l) / \ln(2.2)$ and $n_2 = \ln(l) / \ln(3.3)$.

The point (n_1, n_2) for the foot (0.3048 m) lies on the intersection (-1.5, -1), as shown in Figure 5.

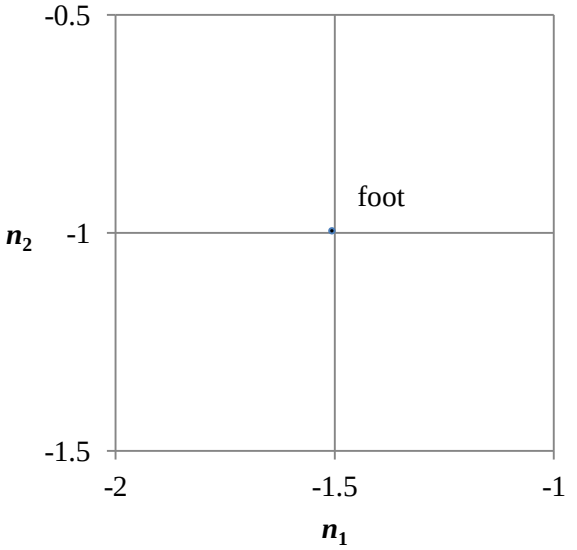

Figure 5: Values of n_1 and n_2 calculated from the length l (in metres) of the foot (0.3048 m), where $n_1 = \ln(l) / \ln(2.2)$ and $n_2 = \ln(l) / \ln(3.3)$.

The value of n_1 for the Bohr radius (5.292×10^{-11} m), an important length-scale in this project [4], equals -30, as shown in Figure 6. The point (n_1, n_2) is located at the intersection (-30, -20).

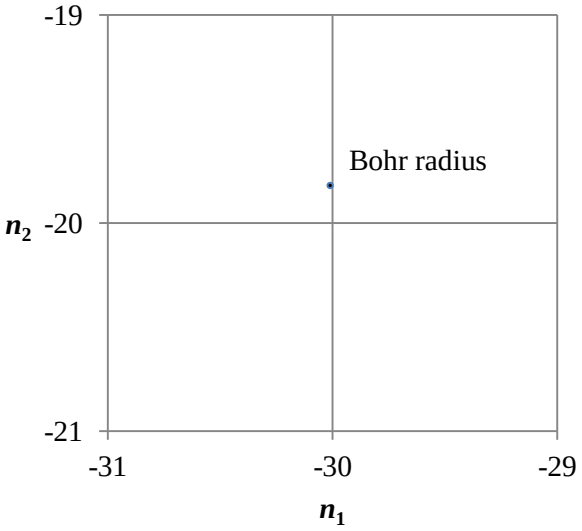

Figure 6: Values of n_1 and n_2 calculated from the length a_0 (in metres) of the Bohr radius (5.292×10^{-11} m), where $n_1 = \ln(a_0) / \ln(2.2)$ and $n_2 = \ln(a_0) / \ln(3.3)$.

The values of n_1 calculated for the two different values of proton RMS charge radius (0.8751(61) fm [5] and 0.8414(19) fm [6]) resulting from different methods of measurement are arranged symmetrically about an integer (-44), as shown in Figure 7. The two points (n_1, n_2) are located at the intersection (-44, -29).

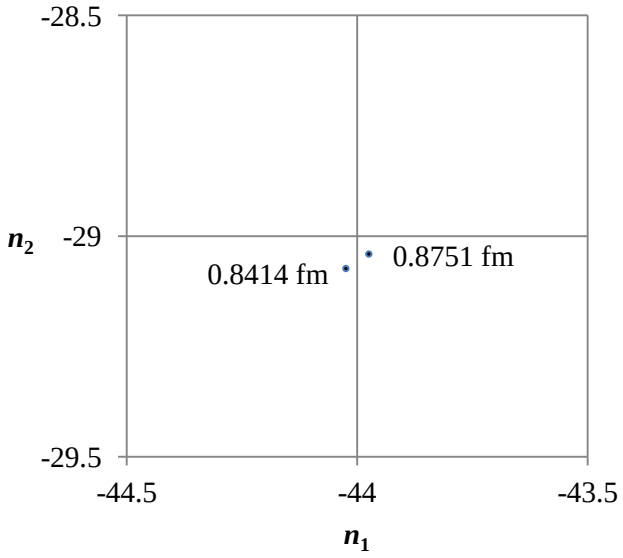

Figure 7: Values of n_1 and n_2 calculated from two values (in metres) of the proton radius r_p (0.8414 fm and 0.8751 fm), where $n_1 = \ln(r_p) / \ln(2.2)$ and $n_2 = \ln(r_p) / \ln(3.3)$.

3 Redshifts of Type Ia Supernovae

An analysis has been made of the redshifts z of the Type Ia supernovae listed in [7]. For the first three supernovae listed, four different pairs of functions have been applied to the data in turn.

First, the functions $f_1(z) = 2200z$ and $f_2(z) = 3300z$ have been applied to the data, resulting in the numbers $n_1 = 2200z$ and $n_2 = 3300z$. The units selected for the graph were 1000 on both axes. The points (n_1, n_2) align with the 'levels' of the graph, as shown in Figure 8. The point (n_1, n_2) for CLA10Cal is located at the intersection (4000, 6000).

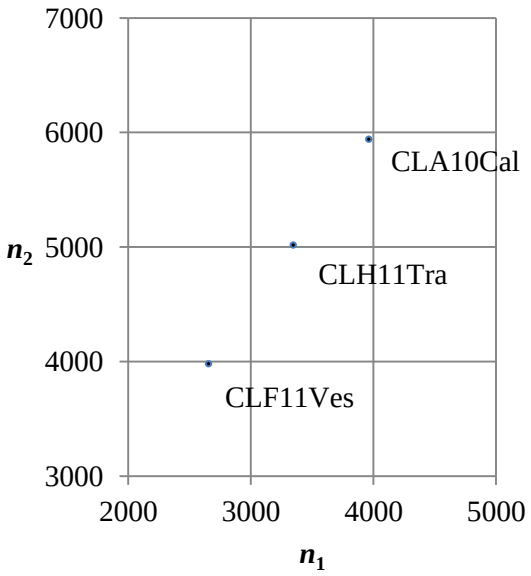

Figure 8: Values of n_1 and n_2 calculated from the redshifts z of the Type Ia supernovae CLA10Cal ($z = 1.800$), CLF11Ves ($z = 1.206$) and CLH11Tra ($z = 1.520$), where $n_1 = 2200z$ and $n_2 = 3300z$.

Two different functions were then applied to the same data: $f_1(z) = 3.53535z$ and $f_2(z) = 4.24242z$. The numbers n_1 and n_2 now take fractional values, as shown in Figure 9.

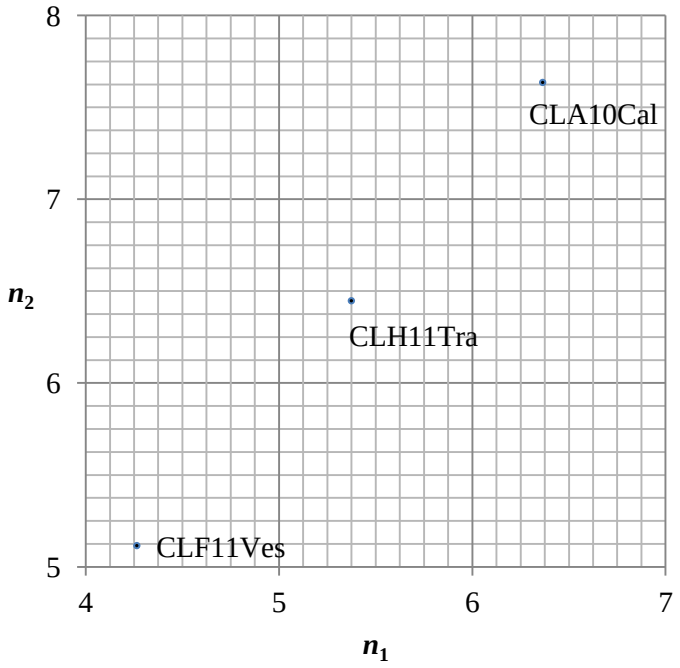

Figure 9: Values of n_1 and n_2 calculated from the redshifts z of the Type Ia supernovae CLA10Cal ($z = 1.800$), CLF11Ves ($z = 1.206$) and CLH11Tra ($z = 1.520$), where $n_1 = 3.53535z$ and $n_2 = 4.24242z$.

Two different functions again were applied to the same data: $f_1(z) = z^3$ and $f_2(z) = z^4$. For each value of z, either n_1 or n_2 takes a fractional value of low denomination, i.e. 2 or 4, as shown in Figure 10.

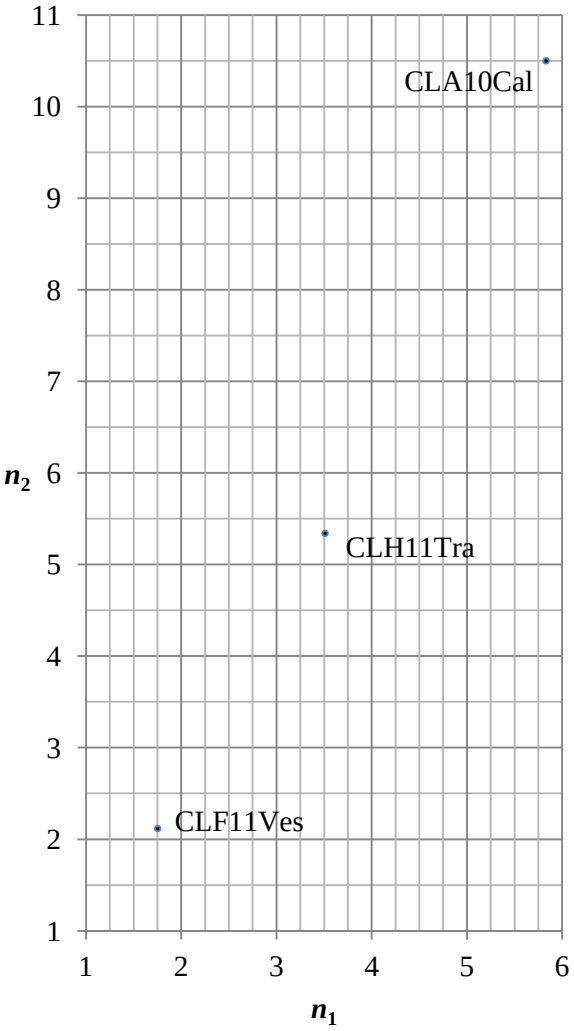

Figure 10: Values of n_1 and n_2 calculated from the redshifts z of the Type Ia supernovae CLA10Cal ($z = 1.800$), CLF11Ves ($z = 1.206$) and CLH11Tra ($z = 1.520$), where $n_1 = z^3$ and $n_2 = z^4$.

Two different functions once again were applied to the same data: $f_1(z) = z^4/4$ and $f_2(z) = z^5/5$. For each value of z either n_1 or n_2 takes a fractional value of low denomination, i.e. 2 or 8, as shown in Figure 11.

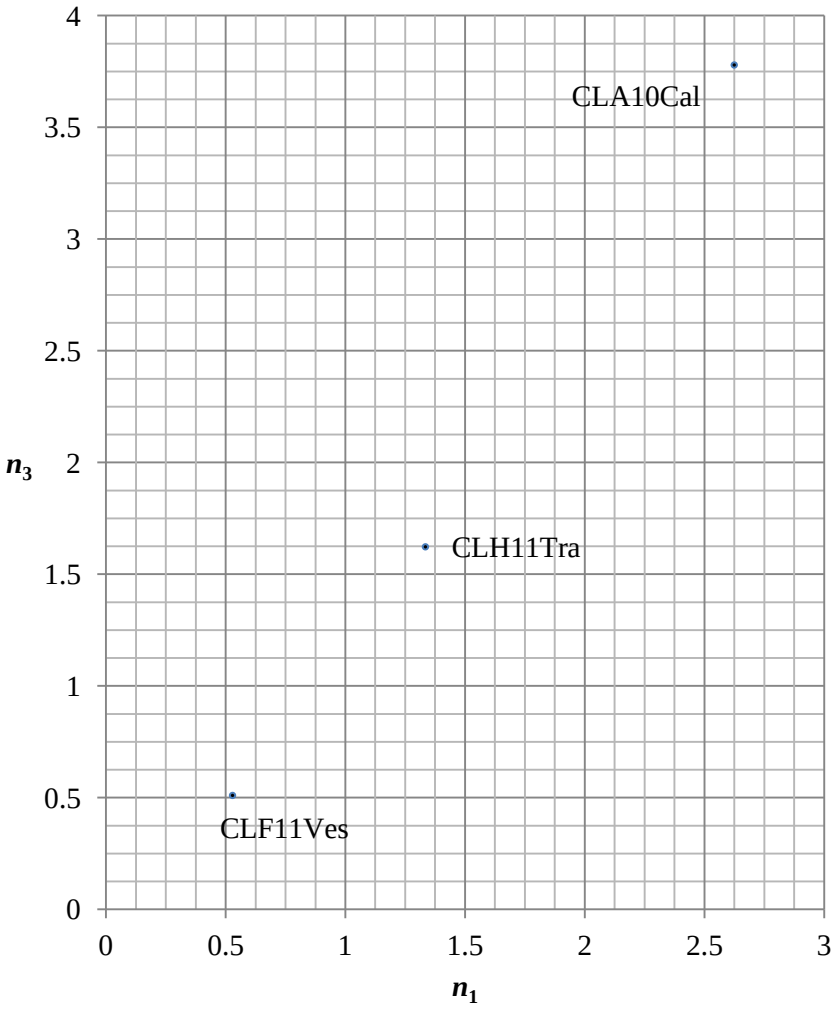

Figure 11: Values of n_1 and n_2 calculated from the redshifts z of the Type Ia supernovae CLA10Cal ($z = 1.800$), CLF11Ves ($z = 1.206$) and CLH11Tra ($z = 1.520$), where $n_1 = z^4/4$ and $n_2 = z^5/5$.

The redshifts of the second three Type Ia supernovae were next analysed. The functions applied to the data were: $f_1(z) = 68.3z$ and $f_2(z) = 46.3z$. The major units selected for the graph are 10 and 5; the minor units are 2.5 and 1.25. The values of n_1 and n_2 lie on or close to the major and minor levels of the graph, as shown in Figure 12.

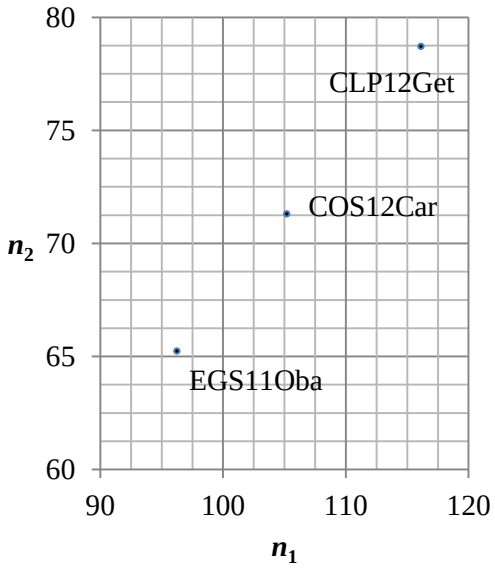

Figure 12: Values of n_1 and n_2 calculated from the redshifts z of the Type Ia supernovae CLP12Get ($z = 1.700$), COS12Car ($z = 1.540$) and EGS11Oba ($z = 1.409$), where $n_1 = 68.3z$ and $n_2 = 46.3z$.

The redshifts of the (four) Type Ia supernovae with the three largest redshifts were next analysed. The functions $f_1(z) = 3.333z$ and $f_2(z) = 4.444z$ have been applied to the data. The numbers n_1 take integer or half-integer values, as shown in Figure 13. The points $(n_1,\ n_2)$ for CLA10Cal and GND13Sto, for which the redshifts are of equal value, lie on the intersection (6, 8).

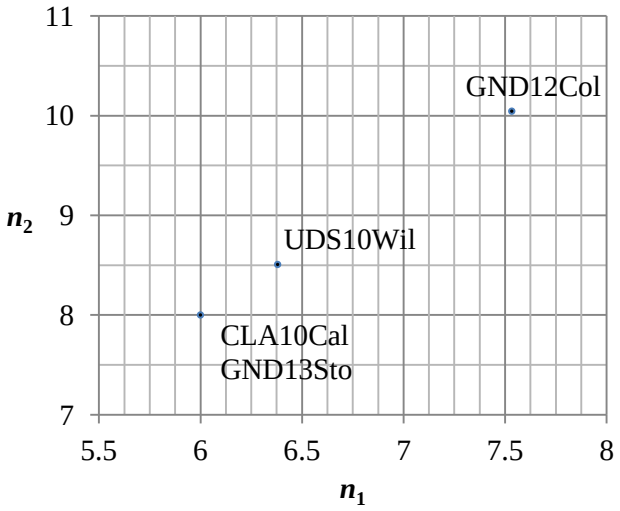

Figure 13: Values of n_1 and n_2 calculated from the redshifts z of the Type Ia supernovae GND12Col ($z = 2.260$), UDS10Wil ($z = 1.914$), CLA10Cal ($z = 1.800$) and GND13Sto ($z = 1.800$), where $n_1 = 3.333z$ and $n_2 = 4.444z$.

Finally, the two Type Ia supernovae with the largest redshifts and the two supernovae with the smallest redshifts were examined. The functions applied to the data were: $f_1(z) = 28.6z$ and $f_2(z) = 88.1z$. The points (n_1, n_2) for the two supernovae with the largest redshifts lie on levels ($n_1 = 55$ and $n_1 = 65$) either side of a major level ($n_1 = 60$), i.e. in a symmetrical configuration, as shown in Figure 14. The points (n_1, n_2) for the two supernovae with the smallest redshifts are arranged symmetrically about a major level ($n_1 = 30$).

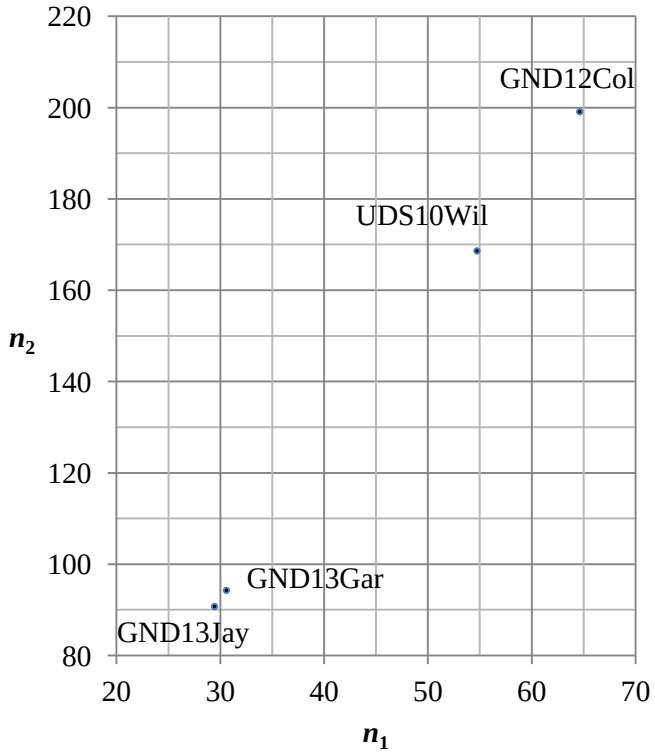

Figure 14: Values of n_1 and n_2 calculated from the redshifts z of the Type Ia supernovae GND12Col ($z = 2.260$), UDS10Wil ($z = 1.914$), GND13Gar ($z = 1.070$) and GND13Jay (z = 1.030), where $n_1 = 28.6z$ and $n_2 = 88.1z$.

4 Random numbers

Three numbers N – only three numbers – between 0 and 100 (71.8188, 50.0911 and 41.3966) were produced using the Excel RAND function. The functions applied to the numbers were: $f_1(N) = N^3/64$ and $f_2(N) = N^4/625$. Major units of 1000 and 5000 were used for the graphs. The point (n_1, n_2) for $N = 50.0911$ lies on a major level at an intersection of major levels, as shown in Figure 15. The point (n_1, n_2) for $N = 71.8188$ lies on a major half-level. The point (n_1, n_2) for $N = 41.3966$ lies on a minor level adjacent to an intersection of major levels.

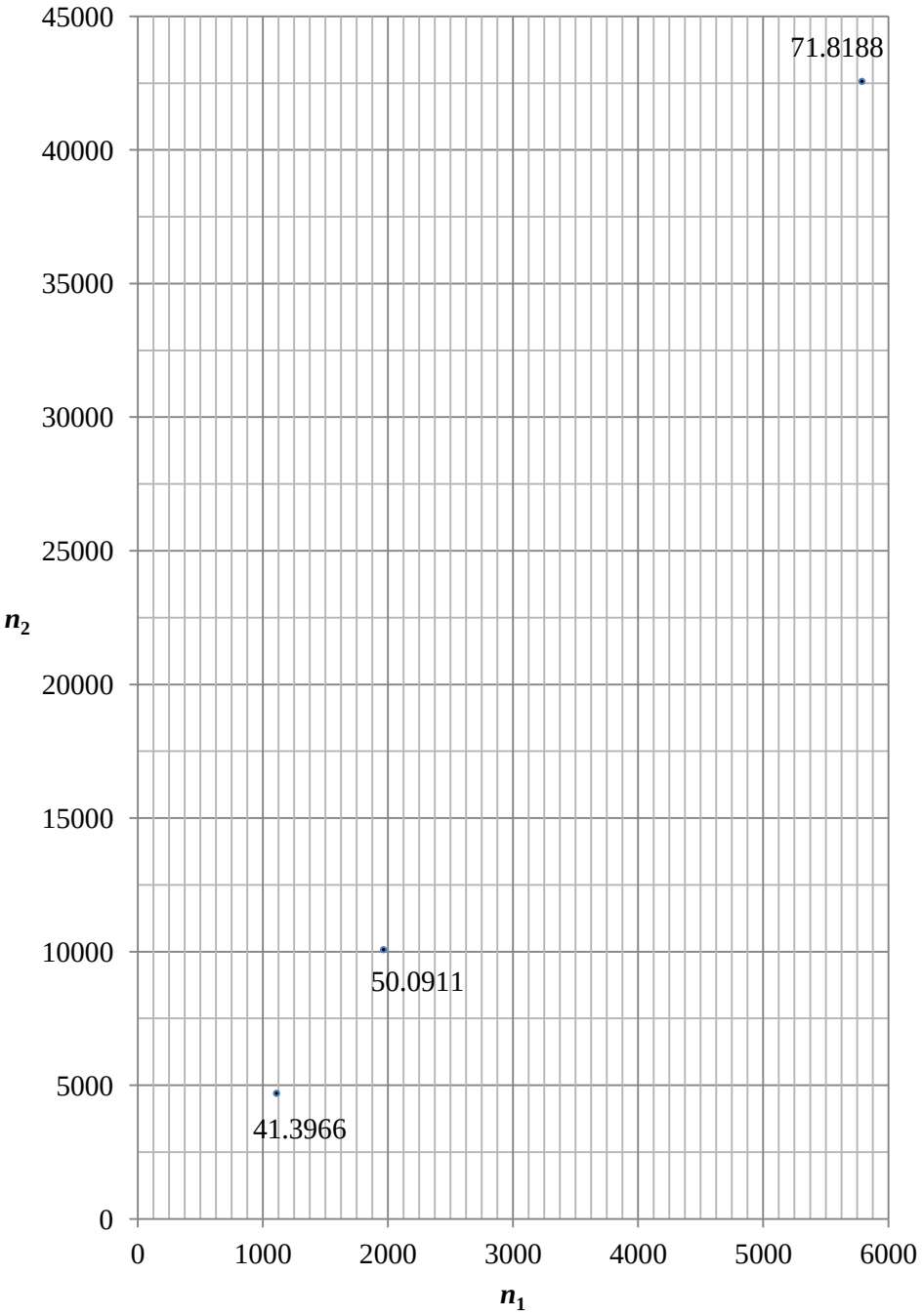

Figure 15: Values of n_1 and n_2 calculated from three random numbers N (71.8188, 50.0911 and 41.3966), where $n_1 = N^3/64$ and $n_2 = N^4/625$.

5 Mean orbital velocities of the planets

The mean orbital velocities of the planets [8] were examined. The functions applied to the data were: $f_1(v) = v/7.7$ and $f_2(v) = v/9.9$, where v is the numerical value of the mean orbital velocity, which was measured in units of km.s^{-1}. The major and minor units of the graph have been chosen as 1 and 1/7 on both axes. The numbers n_1 and n_2 align with integer levels and seventh-integer sub-levels, as shown in Figure 16.

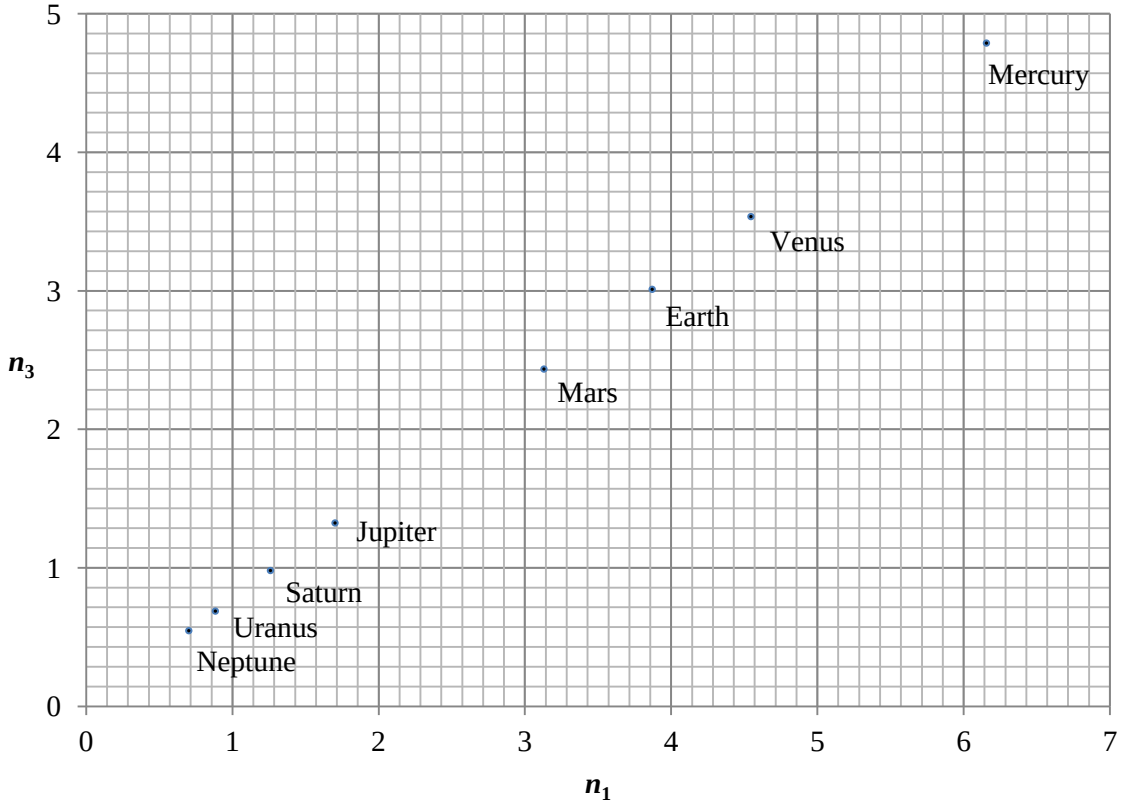

Figure 16: Values of n_1 and n_2 calculated from the numerical values v of the mean orbital velocities, measured in km.s^{-1}, of the solar system planets, where $n_1 = v/7.7$ and $n_2 = v/9.9$. The sub-levels shown are of seventh-integer value.

Mercury	47.4 km.s^{-1}	Jupiter	13.1 km.s^{-1}
Venus	35.0 km.s^{-1}	Saturn	9.7 km.s^{-1}
Earth	29.8 km.s^{-1}	Uranus	6.8 km.s^{-1}
Mars	24.1 km.s^{-1}	Neptune	5.4 km.s^{-1}

6 The source total mass in black hole mergers

For the measurements considered in this section we apply the functions $f_1(M) = \ln(M) / \ln(1.5)$ and $f_2(M) = \ln(M) / \ln(2.5)$, i.e. $M = (1.5)^{n_1}$ and $M = (2.5)^{n_2}$, where M is the numerical value of the source total mass, which was measured in stellar masses $M_\odot$, of a black hole merger event observed by LIGO and Virgo during the first half of the third observing run [9]. The bases 1.5 and 2.5 have been chosen arbitrarily. Five events have been analysed: the first three events; the event with the largest total mass; and the (black hole - black hole) event with the smallest total mass. For the graph the major and minor units have been chosen as 1 and 1/7 on both axes, as in Section 5. The numbers n_1 and n_2 align with integer levels and seventh-integer sub-levels, as shown in Figure 17.

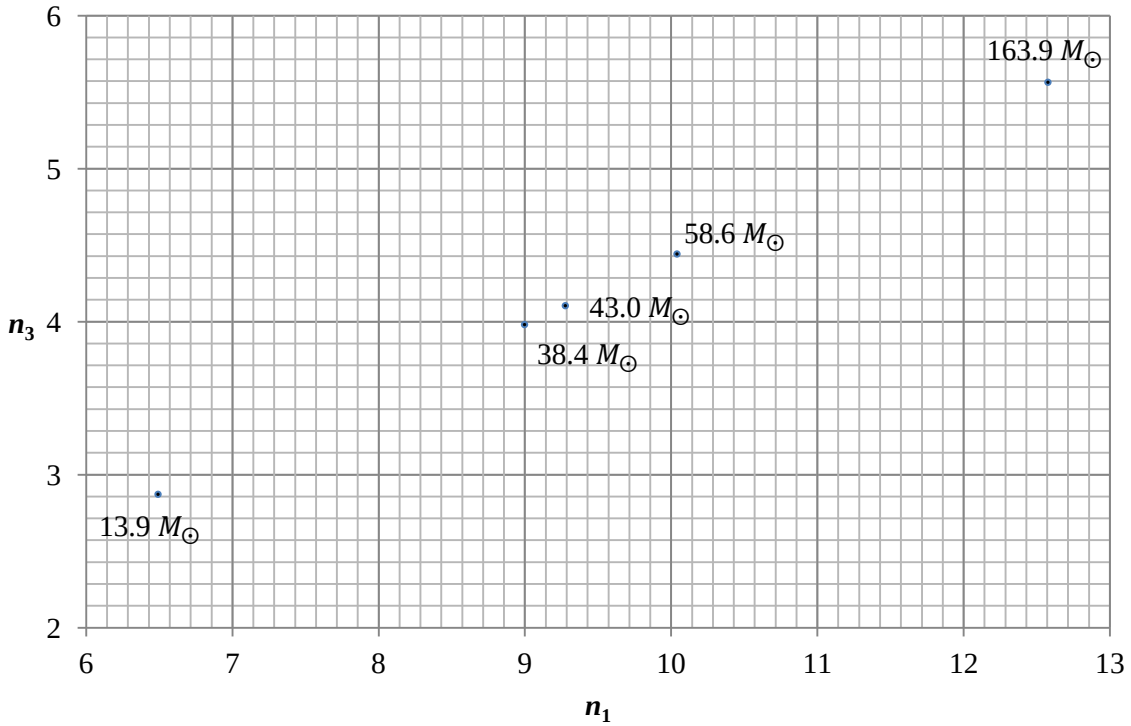

Figure 17: Values of n_1 and n_2 calculated from the source total masses M, in solar masses $M_\odot$, of five black hole mergers observed by LIGO and Virgo during the first half of the third observing run, where $n_1 = \ln(M) / \ln(1.5)$ and $n_2 = \ln(M) / \ln(2.5)$. The sub-levels shown are of seventh-integer value.

Events:	GW190408_181802	43.0 $M_\odot$
	GW190412	38.4 $M_\odot$
	GW190413_052954	58.6 $M_\odot$
	GW190521_	163.9 $M_\odot$
	GW190924_021846	13.9 $M_\odot$

7 Meson masses

For the measurements considered in this section we apply the functions: $f_1(m) = \ln(m) / \ln(2.2)$ and $f_1(m) = \ln(m) / \ln(3.3)$, i.e. $m = (2.2)^{n_1}$ and $m = (3.3)^{n_2}$, where m is the numerical value of a meson mass measured in units of MeV. The same functions were applied to distances and lengths in Section 2. The following mesons have been selected for analysis: $\pi^{\pm}$, $K^{\pm}$, η, ρ, ω, η' and $D^{\pm}$. The major and minor units of the graph have been chosen to be 1 and 1/7 on both axes as in Sections 5 and 6. The numbers n_1 and n_2 align with integer levels and seventh-integer sub-levels, as shown in Figure 18.

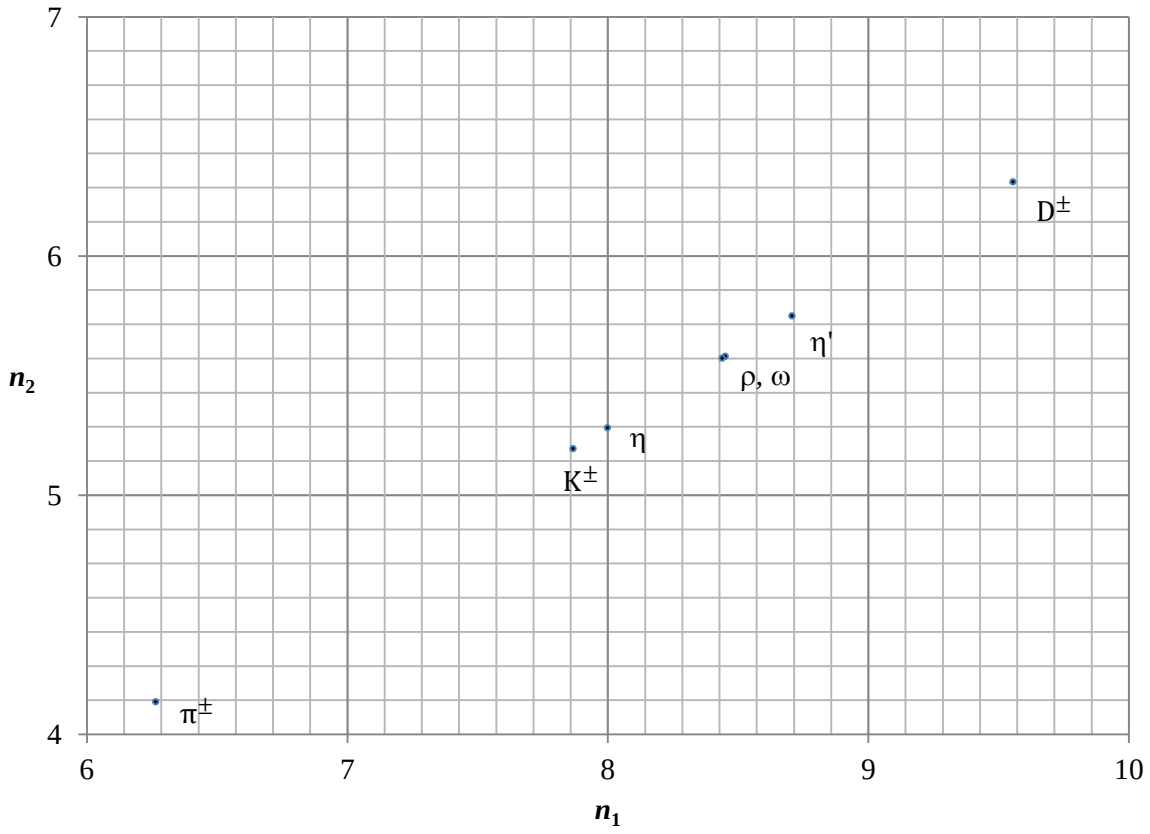

Figure 18: Values of n_1 and n_2 calculated from meson masses m in MeV [10], where $n_1 = \ln(m) / \ln(2.2)$ and $n_2 = \ln(m) / \ln(3.3)$. The sub-levels shown are of seventh-integer value.

$\pi^{\pm}$	139.57 MeV	ω	782.66 MeV
$K^{\pm}$	493.68 MeV	η'	957.78 MeV
η	547.86 MeV	$D^{\pm}$	1869.66 MeV
ρ	775.26 MeV		

8 Discussion

The observer tries to make sense of the world by interpreting measurement outcomes as pure rational numbers and assimilating them into a theory. To do this the observer applies a function of the theory (which in the simplest case, perhaps on a daily basis, is an identity function) to the numerical value of

the measurement outcome which maps it onto a rational number: an integer or a fraction of a denomination chosen by the observer. Mapping to rational numbers is possible since measurement outcomes are subjective to the observer [1, 11, 12]. Integer values suggest a fit to the theory. When several quantities constituting a set are measured the mappings are more likely to be to fractions although integers are favoured first. If powers of 2 are chosen as the denomination of the fractions, half-integers are favoured second, quarter-integers are favoured third and so on. Choosing powers of 2 as the denominations of the fractions spaces the integers and fractions optimally. When two quantities are closely related in the mind of the observer the numerical values of measurement outcomes often map onto symmetrically related numbers. The symmetry may be about a principal level (integer) or sub-level (fraction). In this paper all four examples of closely related quantities (Figures 1, 7 and 14) result in symmetry about principal levels.

The observer can interpret measurement outcomes in accordance with more than one theory. The observer may choose to believe the theory whose functions most commonly map the numerical values of measurement outcomes onto integers. From the totality of measurements the observer apprehends a self-consistent reality ruled by theories believed by the observer.

References

1. B. F. Riley, All measurement outcomes are subjective, viXra:2105.0077
2. https://imagine.gsfc.nasa.gov/features/cosmic/nearest-galaxy-info.html
3. https://www.airmilescalculator.com
4. B. F. Riley, The scales of atomic and particle physics in relation to Planck scale, viXra:1305.0061
5. CODATA 2014
6. CODATA 2018
7. A. G. Riess et al, Type Ia supernova distances at redshift > 1.5 from the Hubble Space Telescope multi-cycle Treasury programs: the early expansion rate, *ApJ* **853** 126 (2018)
8. https://nssdc.gsfc.nasa.gov/planetary/factsheet/
9. The LIGO Scientific Collaboration and the Virgo Collaboration, GWTC-2: Compact binary coalescences observed by LIGO and Virgo during the first half of the third observing run, arXiv:2010.14527v3, Astrophys. J. Lett. **913**, L7
10. P. A. Zyla et al. (Particle Data Group), Prog. Theor. Exp. Phys. 2020, 083C01 (2020) and 2021 update
11. B. F. Riley, Subjective historical timelines, viXra:2102.0112
12. B. F. Riley, The subjectivity of reality, viXra:2104.0041